Supplementary Figures

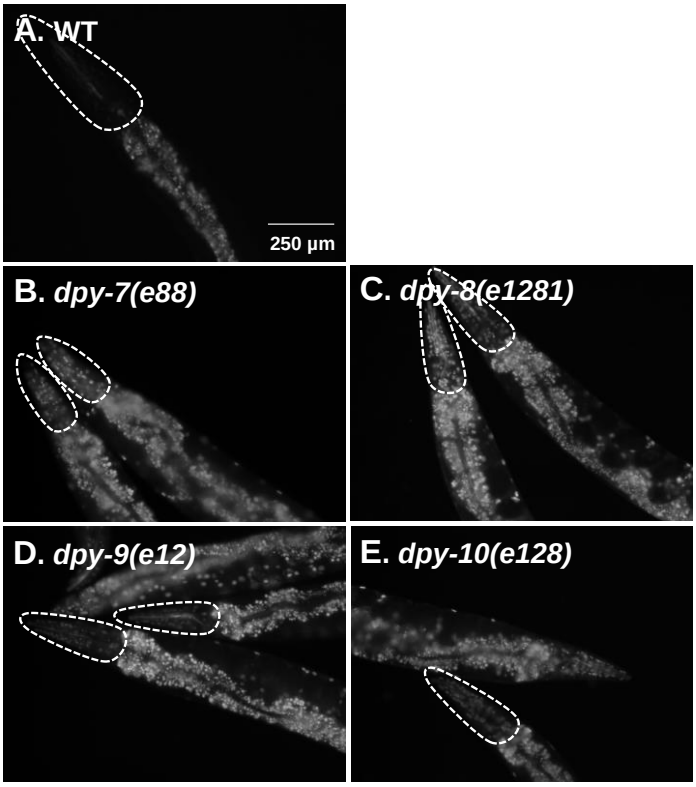

Figure S1. Four collagens encoded in *C. elegans* genome maintain permeability barrier function. Hoechst 33258 staining-based permeability assay of (A) WT, (B) *dpy-7(e88),* (C) *dpy-8(e1281),* (D) *dpy-9(e12), and* (E) *dpy-10(e128)* animals. Scale bar, 250 µm. n=3; N≥10.

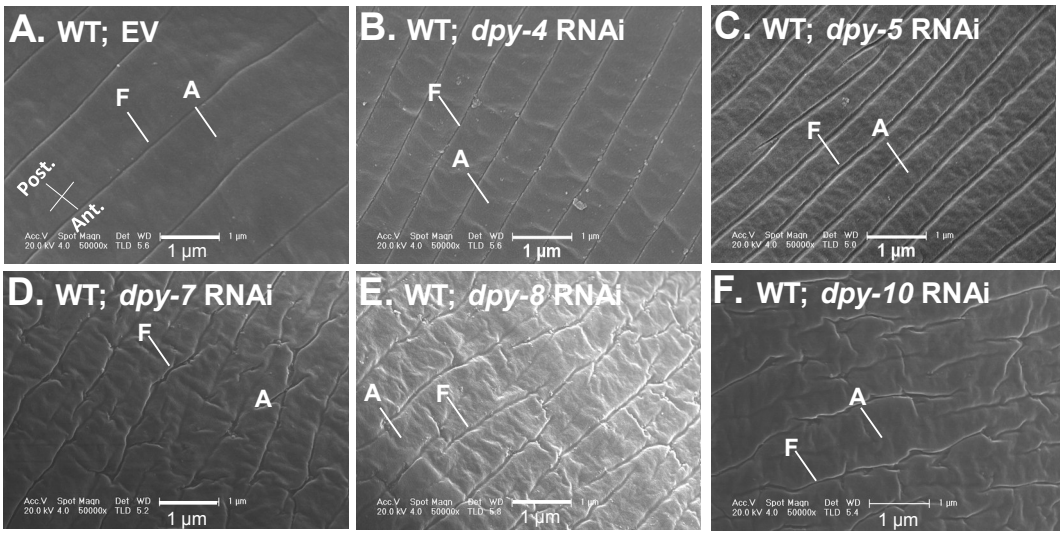

Figure S2. PD collagens maintain the ultra-structure of *C. elegans* cuticle. High resolution scanning electron micrograph of (A) EV, (B) *dpy-4,* (C) *dpy-5,* (D) *dpy-7,* (E) *dpy-8,* and (F) *dpy-10* RNAi animals (50,000x magnification). Annuli, *A*, furrows, *F,* anterior, Ant, and posterior, Post., of worms are indicated. Scale bar, 1 µm.

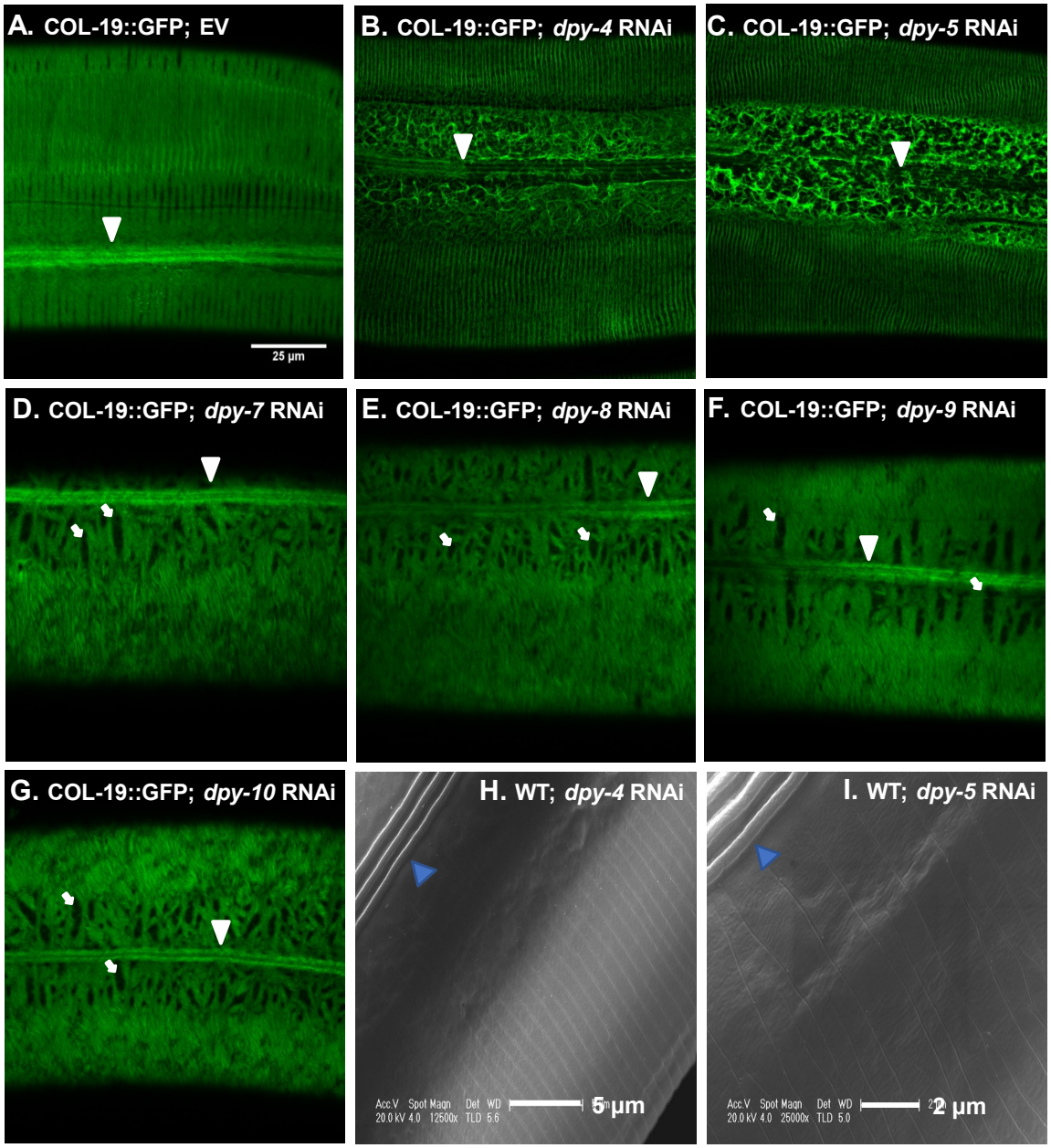

Figure S3. Expression of an adult specific collagen, COL-19, in dumpy animals. P*col-19*::GFP expression and organization in (A) EV, (B) *dpy-4*, (C) *dpy-5*, (D) *dpy-7*, (E) *dpy-8*, (F) *dpy-9,* and (G) *dpy-10* RNAi animals. Arrows in white show GFP free spaces between annuli and arrow heads point to alae. Scanning electron micrographs showing alae (blue arrow heads) in (H) *dpy-4* and (I) *dpy-5* RNAi animals. Scale bar, 25 µm in A-G. Scale bar, 5 µm in H. Scale bar, 2 µm in I.

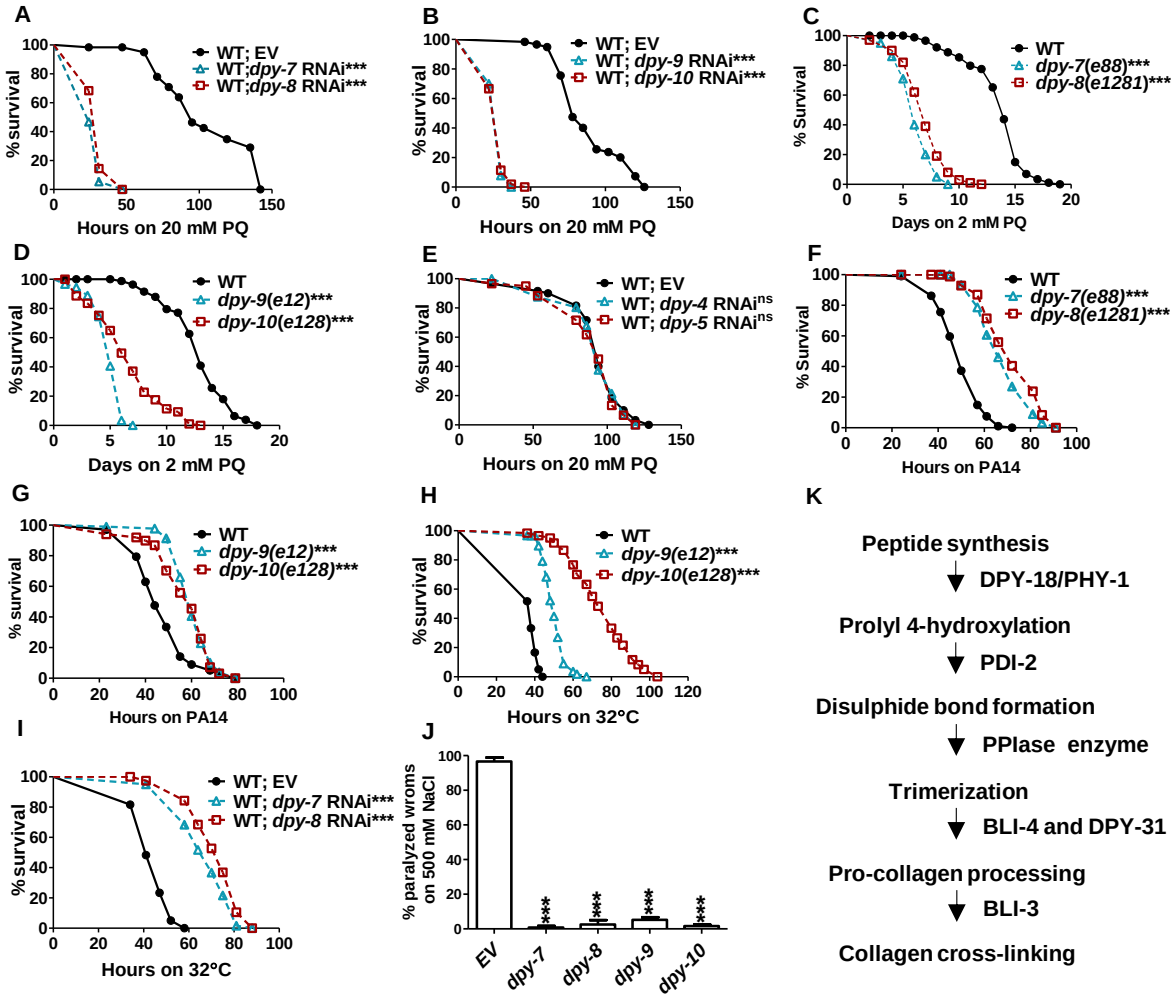

Figure S4. PD collagens regulate survival under biotic and abiotic stresses. Kaplan Meier survival curves of (A) WT animals with EV, *dpy-7* and *dpy-8* RNAi on 20 mM PQ, (B) WT animals with EV, *dpy-9* and *dpy-10* RNAi on 20 mM PQ, (C) WT, *dpy-7 (e88)* and *dpy-8 (e1281)* animals on 2 mM PQ, (D) WT, *dpy-9 (e12)* and *dpy-10 (e128)* animals on 2 mM PQ, (E) WT animals with EV, *dpy-4* and *dpy-5* RNAi on 20 mM PQ, (F) WT, *dpy-7 (e88)* and *dpy-8 (e1281)* animals on *Pseudomonas aeruginosa* PA14 at 25°C, (G) WT, *dpy-9 (e12)* and *dpy-10 (e128)* animals on *Pseudomonas aeruginosa* PA14 at 25°C, (H) WT, *dpy-9 (e12)* and *dpy-10 (e128)* animals at 32°C, (I) WT animals with EV, *dpy-7* and *dpy-8* RNAi at 32°C. n=3; N≥50 for panels A to I. (J) Percent paralyzed of EV, *dpy-4, dpy-5,*

dpy-7, dpy-8, dpy-9, and *dpy-10* RNAi animals upon exposure to 500 mM NaCl. n=3; N≥40. (K) Schematic of collagens processing aided by specific enzymes. *, $p \leq 0.05$; **, $p \leq 0.005$; ***, $p \leq 0.0005$; ns-not significant, $p \geq 0.05$, significance based on Mantel Cox test for survival curves. *p* value for survival curves are indicated next to genotypes. For TD^{50} values in survival assays, see Table S2.

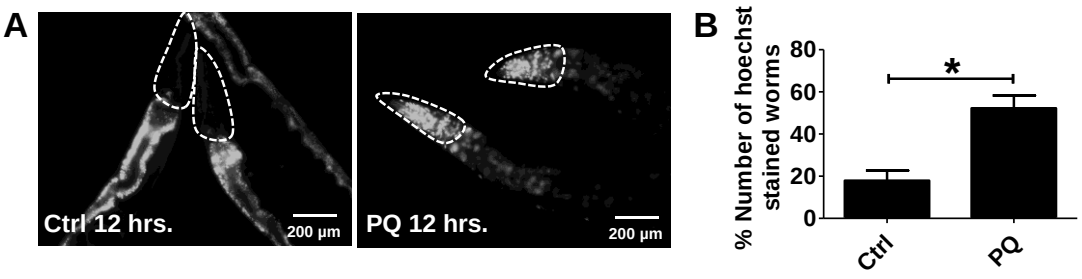

Figure S5. PQ exposure increases cuticle permeability. Hoechst 33258 staining of WT animals exposed to PQ for 12 hours. n=3; N≥15.

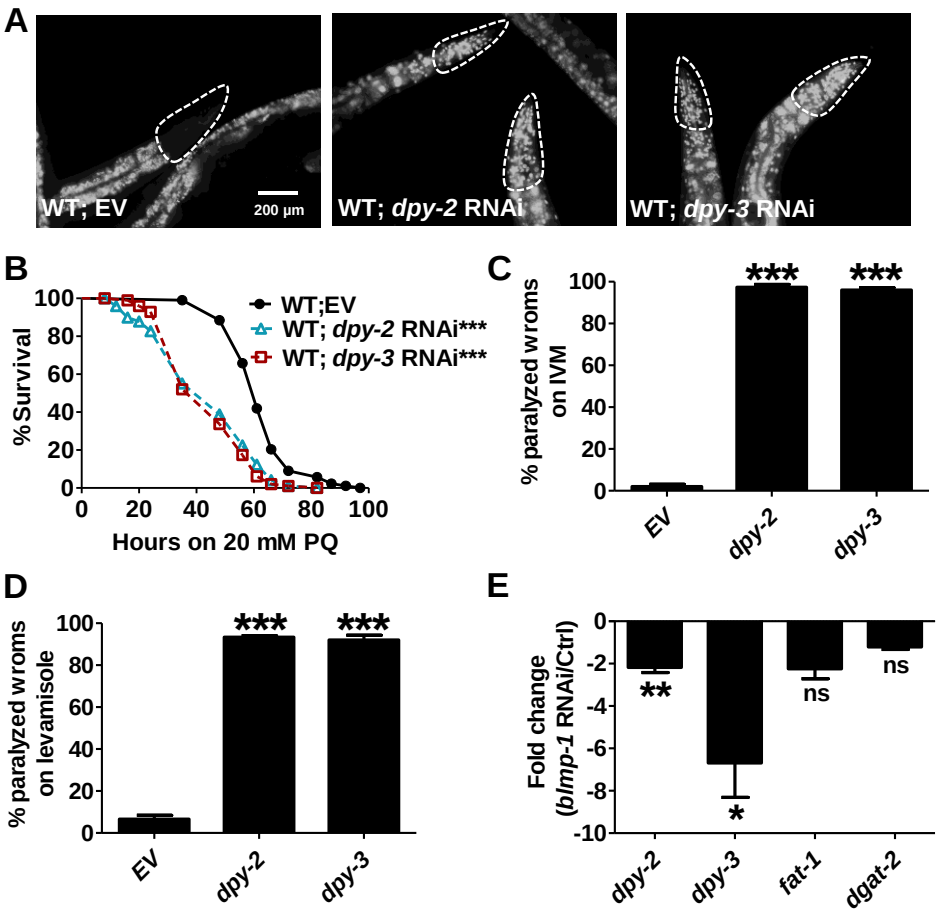

Figure S6. DPY-2 and DPY-3 collagens positively regulate cuticle permeability and survival on exogenous toxins. Hoechst 33258 staining in WT animals with (A) EV, *dpy-2*, and *dpy-3* RNAi. n=2; N=15. Kaplan Meier survival curves of WT animals with (B) EV *dpy-2*, and *dpy-3* RNAi on 20 mM PQ. Percent paralyzed of WT animals with EV, *dpy-2, and dpy-3* RNAi upon (C) 50 µM Ivermectin (IVM) and (D) exposure to 125 µM levamisole. n=3; N≥50 for panels C and D. qRT-PCR analysis transcripts for collagens and lipid metabolism enzymes, fatty acid desaturase *fat-1* and diacylglycerol acyl transferase *dgat-2*, upon (E) *blmp-1* RNAi *in* WT animals. Error bars indicates SEM. *, $p \leq 0.05$; **, $p \leq 0.005$; ***, $p \leq 0.0005$; ns-not significant, $p \geq 0.05$, significance based on Mantel Cox test for

survival curves. *p* value for survival curves are indicated next to genotypes. For TD^{50} values in survival assays, see Table S2.

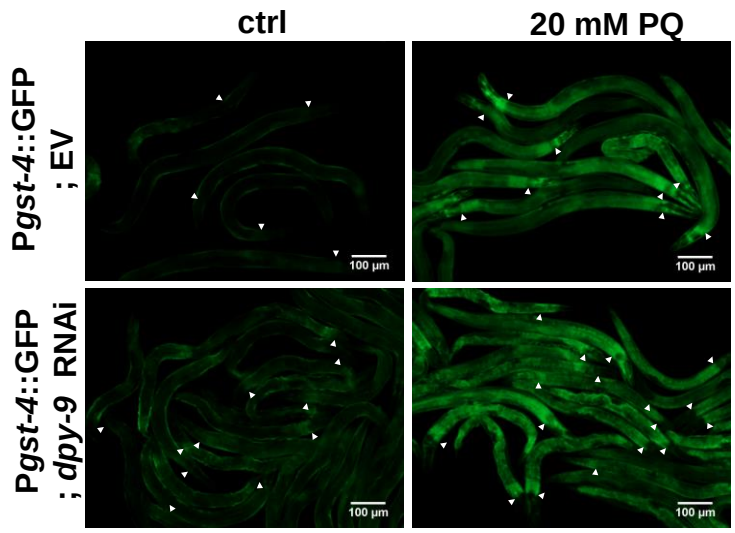

Figure S7. *dpy-9* animals show robust induction of GST-4. *gst-4*p::GFP induction in EV and *dpy-9* RNAi animals upon exposure to 20 mM PQ for 6 hours. Arrow heads indicates pharynx and intestine junction.

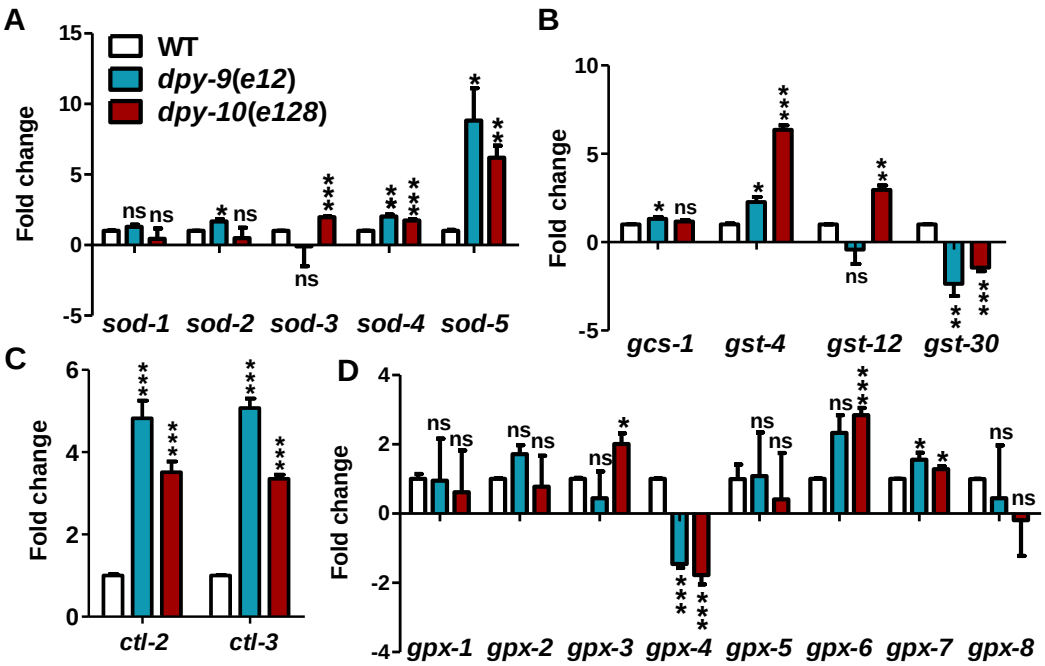

Figure S8. *dpy-9* and *dpy-10* animals show high basal expression of antioxidants. Histograms showing qRT-PCR analysis of (A) superoxide dismutases (*sod*s), (B) gamma-glutamylcysteine synthetase (*gcs-1*) and glutathione synthetases (*gst*s), (C) catalases (*ctl*s), and (D) glutathione peroxidases (*gpx*s) in WT, *dpy-9 (e12)* and *dpy10 (e128)*. Error bars indicates SEM. *$p \leq 0.05$, **$p \leq 0.005$, ***$p \leq 0.0005$, ns-not significant, students *t* test.

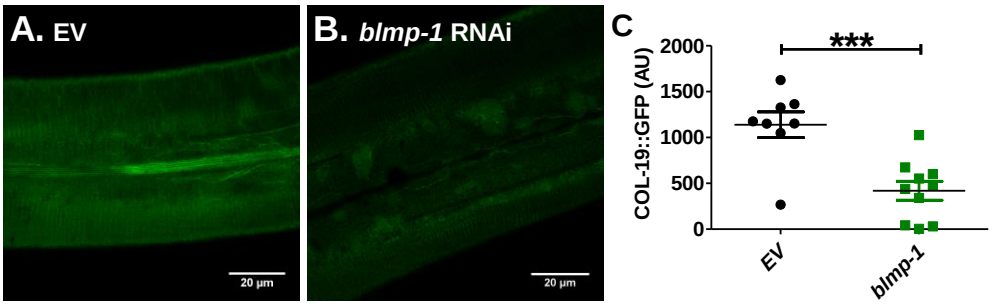

Figure S9. BLMP-1 regulates COL-19 expression. P*col19*::GFP expression in (A) EV and (B) *blmp-1* RNAi animals. (C) Quantification of COL-19::GFP expression in EV and *blmp-1* RNAi animals. Error bars indicates SEM. **p*≤ 0.05, ***p*≤ 0.005, ****p*≤ 0.0005, ns-not significant, significance based on students *t* test. Scale bar, 20 µm.

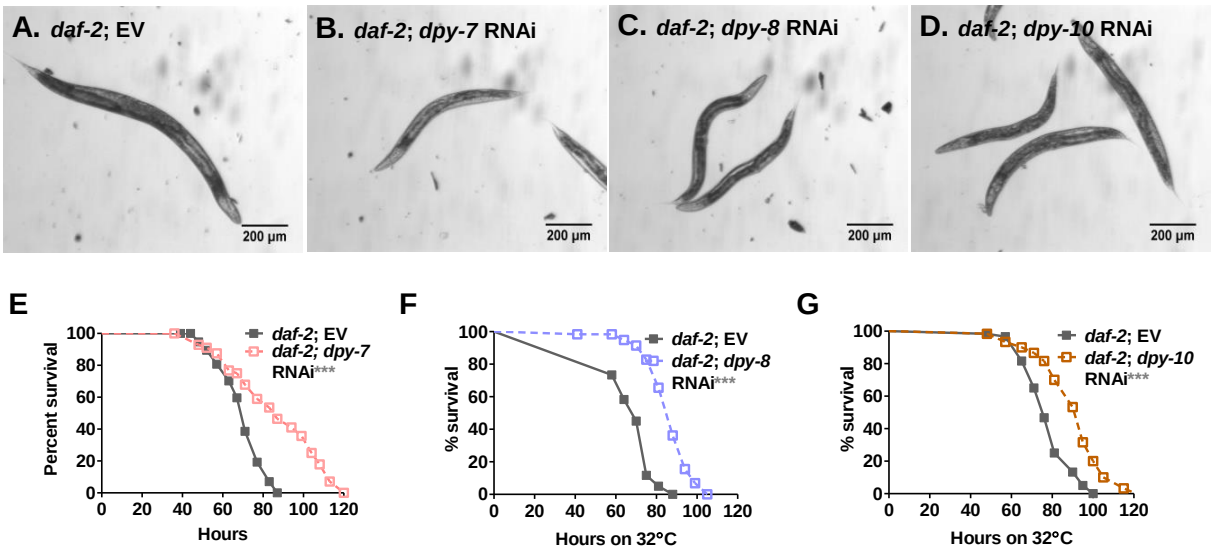

Figure S10. PD collagens do not affect thermal stress resistance of *daf-2* animals. Images of *daf-2 (e1370)* animals with (A) EV, (B) *dpy-7*, (C) *dpy-8* and (D) *dpy-10* RNAi. Kaplan Meier survival curves of EV control and (E) *dpy-7,* (F) *dpy-8,* (G) *dpy-10* RNAi in *daf-2 (e1370)* animals in thermal stress assay at 32°C. n=3; N≥50 for panels E to G. *, $p \leq 0.05$; **, $p \leq 0.005$; ***, $p \leq 0.0005$; ns-not significant, $p \geq 0.05$, significance based on Mantel Cox test for survival curves. *p* value for survival curves are indicated next to genotypes. For TD^{50} values in survival assays, see Table S2.